Absolute frequency of cesium 6*S*–8*S* 822 nm two-photon transition by a high-resolution scheme

Chien-Ming Wu,[1,2] Tze-Wei Liu,[2] Ming-Hsuan Wu,[2] Ray-Kuang Lee,[1] and Wang-Yau Cheng[2,*]

[1]*Institute of Photonics Technologies, National Tsing Hua University, Hsin-Chu 30013, Taiwan*

[2]*Department of Physics, National Central University, Chun-Li 32001, Taiwan*

**Corresponding author: wycheng@ncu.edu.tw*

Received May 23, 2013; revised July 8, 2013; accepted July 8, 2013;
posted July 9, 2013 (Doc. ID 190999); published August 15, 2013

We present an alternative scheme for determining the frequencies of cesium (Cs) atom 6*S*–8*S* Doppler-free transitions. With the use of a single electro-optical crystal, we simultaneously narrow the laser linewidth, lock the laser frequency, and resolve a narrow spectrum point by point. The error budget for this scheme is presented, and we prove that the transition frequency obtained from the Cs cell at room temperature and with one-layer μ-metal shielding is already very near that for the condition of zero collision and zero magnetic field. We point out that a sophisticated linewidth measurement could be a good guidance for choosing a suitable Cs cell for better frequency accuracy.

OCIS codes: (120.3940) Metrology; (300.6210) Spectroscopy, atomic; (300.3700) Linewidth; (270.1670) Coherent optical effects.

http://dx.doi.org/10.1364/OL.38.003186

Absolute frequencies of the cesium (Cs) atom $S \rightarrow S$ Doppler-free transitions offer an excellent basis for testing fundamental principles in physics, such as QED verification [1] via frequency comparison with the hydrogen atom, the parity nonconservation calculation [2], and possible quark mass variation [3] using the feature of the heavy Cs nucleus. For metrology applications [4,5] the Cs 6*S*–8*S* two-photon stabilized 822 nm diode laser, of which a hand-size version was recently demonstrated [4], could become a very convenient secondary optical frequency standard because of its excellent spectral features [5] as well as the flexibility of being calibrated by a 411 nm Yb^+ clock [6]. Two research groups have tried to obtain the transition frequencies by very different approaches [1,7], namely, "direct comb laser spectroscopy" and "frequency chain." We here demonstrate a third approach for obtaining new frequencies of the two Doppler-free 6*S*–8*S* transitions with 1 order of magnitude higher precision over the latest published measurement [1]. The accuracy of the transition frequency is discussed after we have inspected ten Cs cells. We suggest the frequency to be determined from the cells that yield the Lorentian-part linewidth near the theoretical natural linewidth.

Figure 1 shows a simplified block diagram of our experimental design, which allowed us to simultaneously achieved the following three primary tasks of narrowing the laser linewidth, stabilizing the laser frequency, and scanning the laser carrier frequency for high-precision spectroscopy. The extended cavity diode laser (ECDL) system (Fig. 1) served as the master laser [5] in this experiment. The output light after a tapered amplifier (TA) was sent to a spatial filter, and then a 200 mW spatially regulated laser beam was split equally into the electro-optical modulator (EOM) area and acoustic-optical modulator (AOM) area in which the time base of the two modulator's drivers were all phase locked against the time base of a Cs clock. The EOM area is set up for both laser stabilization and laser carrier frequency (ω_c) scanning. The driving frequency of the EOM is provided by a function generator (Agilent 81150A) that allows us to dither the EOM modulation frequency (Δ_0) with an external dither source (ω_d, Agilent 33250A). Consequently, the optical phase (ϕ) was modulated as $\phi = M \cos \Delta t$ with a dither frequency ω_d embedded in the modulation frequency Δ, that is, $\Delta = \Delta_0 + A \cos \omega_d t$. Here, a modulation index (MI) of 0.4 rad is used; Δ_0 is 106 MHz; A is 1 MHz; ω_d is 28 kHz. Dithering the EOM frequency was for obtaining a first-derivative spectrum from Cs cell #1 (81°C wall temperature). The smooth curve on the center of the Pound–Drever–Hall (PDH) signal (green dashed inset, Fig. 1), for reducing laser jitter to 20 kHz bandwidth, proves an interesting fact that the aforementioned dither on sidebands was just canceled out in the heterodyned PDH signal. That is, dither

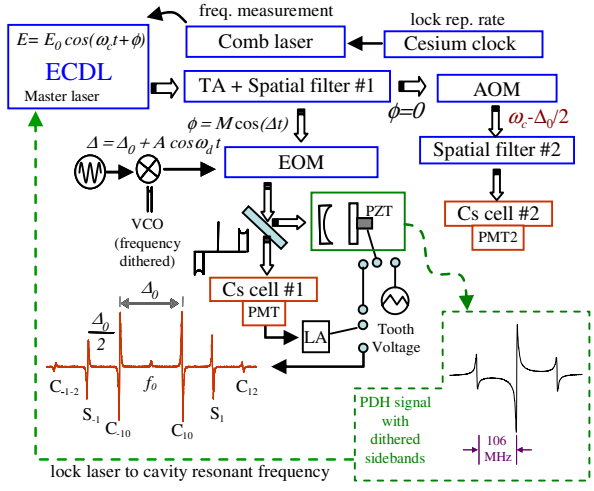

Fig. 1. Simplified block diagram for simultaneously narrowing laser linewidth, stabilizing laser carrier frequency by cell #1, and resolving unperturbed two-photon spectrum by cell #2. ECDL, extended cavity diode laser; EOM, electro-optical modulator (modulation depth $M = 0.4$ rad); AOM, acousto-optical modulator; S_n, sideband induced spectrum; C_{nm}, crossover (see text); TA, tapered amplifier; VCO, voltage controlled oscillator; LA, lock-in amplifier; PMT, photomultiplier. Note that no dither influence was found from the center of the Pound–Drever–Hall (PDH) signal.

sidebands would not influence the PDH locking. A sawtooth voltage was applied to the PZT of the reference cavity to control the laser frequency to resolve the entire derivative spectrum, as displayed in red color in Fig. 1. Note that all the spectral components are from the same optical transition ($F = 3 \rightarrow F' = 3$). When the cavity resonance frequency reaches a spectral component of interest, the sawtooth voltage is suspended, and the derivative spectrum is used to stabilize the cavity length, which in turn stabilizes the master laser frequency.

The obtained Doppler-free derivative spectrum (Fig. 1) consists of seven components, which, basically, are formed by three different sorts of mechanisms: S_n is resolved by sidebands; C_{nm} is the crossover of the nth sideband and mth sideband (0 stands for carrier); and f_0 is induced by the carrier and is not supposed to appear at the output of the lock-in amplifier. Nevertheless, a small bump appears at the frequency position of f_0. This bump is caused by the inhomogeneous dither on the sideband, leading to a tiny residual amplitude modulation on the fluorescence. We find that C_{-10} line is superior to the S_{-1} line for laser stabilization; this is because, first, we thus do not need a high MI for an optimized signal-to-noise ratio (S/N), which greatly reduces the pain of applying a homogenous and high RF power on our home-built EOM crystal. In other words, compared to that of S_{-1} line, only 0.14 of the RF power is needed to optimize the S/N of the C_{-10} line; second, the C_{-10} line suffers from less amplitude modulation and modulation shift than does the S_{-1} line when the MI is smaller than 1 [8]. Note that any frequency offset from the Cs cell #1 system will not influence our obtained frequency value, which is independently determined by the Cs cell #2 system, since the carrier frequency of the master laser is always monitored by a self-reference Ti:sapphire comb laser during the period of data acquisition. We refer the comb laser repetition rate to a Symmetricom 5071A Cesium clock, whose frequency was traced to UTC (TL) [9] via the flying clock method, which resulted in 1.4×10^{-14} one-day accuracy and 10^{-11} for a 10 s sampling time.

The AOM area is for shifting the laser carrier frequency to be on resonance with some spectrum component of interest and for regulating the light intensity in Cs cell #2. Light fluctuation in Cs cell #2 is then suppressed to a 0.2% intensity ripple (100 kHz bandwidth). We very carefully overlapped the waists between the forward and the retroreflected beams on the pinhole of spatial filter #2 to reduce the influence of imperfect wavefront overlapping. When we designedly misaligned the counterpropagating beams so that the fluorescence height decayed to half-magnitude; a 1.7 kHz frequency shift was observed. Therefore, the frequency error due to imperfect wavefront overlapping could be estimated as smaller than 0.3 kHz based on the best beam adjustment we could achieve. The laser beam was loosely focused to Cs cell #2 such that the Rayleigh range could be longer than the fluorescence detection area. Consequently, a 0.2 mm diameter (e^{-1}) waist located on the center of Cs cell #2 was produced.

The spectral profile from Cs cell #2 could be displayed by stepwise variation of the Δ_0 of the EOM (Fig. 1), where the AOM frequency was set to $\Delta_0/2$ and the -1 order was used so that the crossover line retrieved from Cs cell #1 could be used for laser stabilization. Figure 2 presents a typical spectrum of the Cs $6S \rightarrow 8S$ Doppler-free transition that was recorded from a lock-in amplifier output of the Cs cell #2 system in which the laser beam was chopped by the AOM in Fig. 1. Note that the AOM frequency is fixed during data acquisition. The AOM frequency yields an accuracy of better than 0.1 Hz. Each data point was taken with 8 s sampling time, and each frequency step was 100 kHz. The error bar in Fig. 2 is smaller than the red dot data, magnified in the inset for comparison. The peak residual is 1.5×10^{-2}, and the average value of residual is 2×10^{-5}, relative to the signal peak height. Under a fixed laser power, the average peak position of a line in the spectrum was determined by recording the same line nine times. We found that either repeating Fig. 2 nine times with a 100 kHz/step, or tracing the spectrum with a 10 kHz/step once, would provide almost the same peak value and the same fitting uncertainty, and the highly symmetric fitting residual led to a 300 Hz peak fitting uncertainty. The black fitting curve in Fig. 2 is the convolution of Lorentian and double-exponential (transit-time) line shape [7,10], resulting in 932 kHz width in the Lorentian part and 466 kHz transit-time broadening, which is consistent with the theoretical natural linewidth (920 kHz) [1]. We fitted the linewidth with ten Cs cells, and they yield almost the same transit-time width, because we only replace Cs cell for each inspection.

The reason that we did not phase lock the frequency of our master laser to the comb laser to stepwise resolve a spectrum like that produced in Fig. 2 is that one commercial Cs clock is not sufficient to provide a short-term accuracy without the help of a H-maser. Hence, master laser stabilization by the aforementioned derivative spectrum is vital and is an economic approach (comparing with using a H-maser) to reducing the error bar of each data point in Fig. 2.

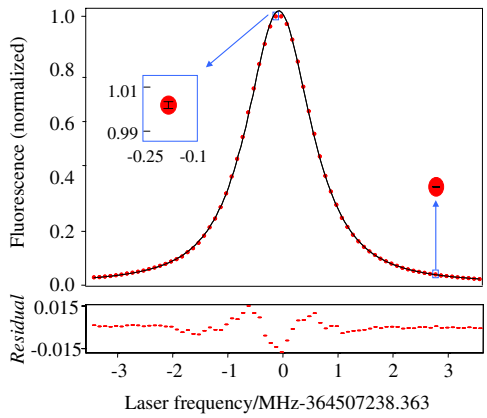

Fig. 2. Typical spectrum of the cesium (Cs) $6S$–$8S$ hyperfine transition and the fitting residual (all normalized to peak height), from cell 2; the EOM sideband frequency is locked to C_{-10} line. Insets show the size of error bars relative to red dot. Black line, Lorentz-transit-time fitting [10] with 1.36 MHz total width FWHM. Cell wall temperature, 23°C; laser power in the middle of cells (waist), 120 mW/mm^2. Note that the fitting residual is symmetric and that the real scale is much smaller than that in the figure.

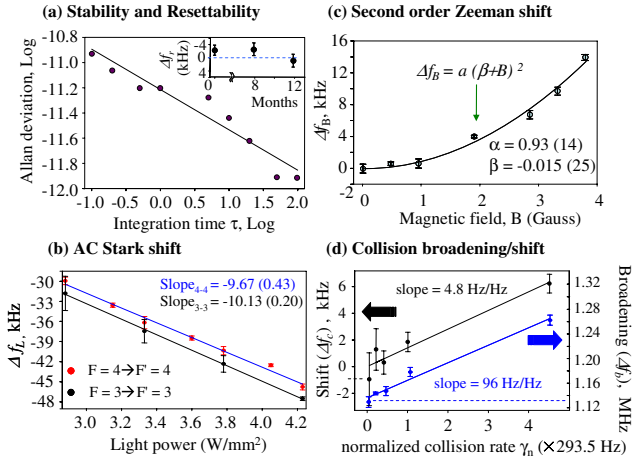

Fig. 3. Error budget for determining the absolute frequency of Cs $6S$–$8S$ hyperfine transitions (a) Two sample Allan deviations (comb laser beat against master laser); inset, resettability (Δf_r, relative to mean value). Log scale on both axes. (b) Typical light shift at room temperature, relative to statistical zero-light-intensity frequency (Δf_L); "Light power" means total laser power per area in the waist (center of cell). (c) Longitudinal magnetic field (by solenoid current) versus frequency shift: β, residual magnetic field; Δf_B, frequency deviation from zero current; black solid line, $\Delta f_B = \alpha(\beta+\beta)^2$ where β is the fitted residual field. (d) Collision shift and broadening; see text.

Figure 3 illustrates other error budget for extrapolating the absolute frequency. The inset in Fig. 3(a) displays one-year absolute frequency variation, and a resettability of 3.4 kHz (standard deviation) is concluded. Between the first and second data acquisition period, the entire laboratory was moved 49 km, and we rebuilt the experiment with the laser beam waist twice the original size. The main part of Fig. 3(a) displays a typical Allan deviation, which was obtained from the beat note between the master laser and one mode of the comb laser. The short-term frequency variation Δf_A, about 2 kHz at 10 s sampling time, is attributed to the short term instability of the Symmetricom 5071A Cesium clock, because the master laser in Fig. 1 yields a much smaller frequency variation, i.e., around 300 Hz at 10 s sampling time, as was proved in [7]. Figure 3(b) shows the typical light shift with the shift (Δf_L) relative to the extrapolated zero-light frequency. The maximum statistical error fitting to the zero-light frequency is 1.7 kHz. Different slopes of light shifts were observed for the different hyperfine components, and that would be helpful for understanding the S-state hyperfine-dependent quadrupole structure of the Cs atom [11]. Note that different quantum efficiency of detectors and different definitions of beam size [12] might lead to different values of the light shift, although it would not influence the value of the fitted zero-light frequency as we have experimentally confirmed. Figure 3(c) shows that the residual Zeeman shift is small ($\alpha * \beta^2 = 0.2$ Hz). Figure 3(d) illustrates our results for studying the collision shift Δf_c (relative to the zero collision) and collision broadening Δf_B. The collision rate is proportional to γ, which equals $\sigma_{\text{eff}} \times n_{id} \times V_{\text{ave}}$, where σ_{eff} means effective collision, n_{id} means atomic density for ideal gas and V_{ave} is the mean atomic speed. We introduce the normalized collision rate γ_n as

Table 1. Obtained Frequencies of ^{133}Cs 8S Hyperfine Levels

	[a] $F = 3-3$ (kHz)	[b] $F = 4-4$ (kHz)	Hyperfine Constant (kHz)
Ref. [1]	417 (15)	351 (15)	219,124 (7)
This work	363 (10)	297 (10)	219,124 (7)
Ref. [7]	320 (100)	260 (100)	219,120 (10)

[a] +364, 507, 238, 000 kHz.
[b] +364, 503, 080, 000 kHz.

$\gamma_n = \gamma/\sigma_{\text{eff}} = (P_{\text{vapor}}/RT_{\text{wall}}) \times (8RT_{\text{wall}}/\pi M)^{0.5}$, where T_{wall} means wall temperature. From Fig. 3(d) we found that the measured room-temperature frequency and linewidth are almost the same as the values of the extrapolated zero collision. This finding confirms the room-temperature approximation used in [1]. The statistical errors in Figs. 3(b)–3(d) contribute to the resettability of Fig. 1(a). All the extrapolations and the error budget in Fig. 3 are only for a specific cell and are not enough to ensure accuracy. Hence, examining more cells from different sources would help determine the transition frequencies more accurately. We examined ten cells, and all the cells yielded similar resettability within four months, including one cell with 10 Pa Xe buffer gas. To our surprise, the differences of the obtained absolute frequencies scattered over 400 kHz! Moreover, the broadest linewidth from the cells with no buffer gas can be 1.7 times wider than the narrowest one, while 2% variation in linewidth was distinguishable in our scheme. Thus, we find an interesting tendency that the absolute value of the frequency deviations from that of the narrowest linewidth monotonically increases with their spectral widths, and we determined the absolute frequencies from the cells for which the fitted Lorentian-part linewidth (narrowest) is consistent with the theoretical natural linewidth. We quoted 10 kHz error, instead of the resettability measurement (3.4 kHz) in Fig. 3(a), upon considering that there might be other unknown facts from the other cells.

Table 1 list the comparisons between our results with previous results, where the hyperfine constant is deduced as (clock frequency $-2\Delta\nu_m$)/$F_{\max}$; $\Delta\nu_m$ is the difference of the measured two fundamental frequencies, and $F_{\max}$, is the largest total angular momentum and is 4 in our case. We find that the frequency difference of the obtained values of two different hyperfine transitions is in very good agreement with the previous experiment (the same value), but the absolute frequencies are quite different. The discrepancy between our work and previous work might be caused by the interaction with different cell walls [13] (including the tiny outgassing), from which the interaction can lead to the line-shape broadening. In addition, it is interesting to clarify, under the same laboratory conditions, whether peak power plays a role in the discrepancy, since two experiments performed with a CW laser [7] yielded different results from those with a pulse laser [1].

We are grateful to Mr. Shinn-Yan Lin at Telecommunication Laboratories, who provided us the Cs atomic clock; Dr. Thomas Udem at MPQ (Max Planck Institute

for Quantum Optics) for sophisticated revision of the manuscript; Prof. J.-T. Shy for valuable comments; the AMO focus group of National Science Council (NSC); and the CQSE of National Taiwan University, who offered nice platforms for useful research communications. This research was supported by NSC with contract 101-2112-M-008-009.

References

1. P. Fendel, S. D. Bergeson, Th. Udem, and T. W. Hansch, Opt. Lett. **32**, 701 (2007).
2. A. Derevianko and S. G. Porsev, Eur. Phys. J. A **32**, 517 (2007).
3. T. H. Dinh, A. Dunning, V. A. Dzuba, and V. V. Flambaum, Phys. Rev. A **79**, 054102 (2009).
4. Y.-H. Chen, T.-W. Liu, C.-M. Wu, C.-C. Lee, C.-K. Lee, and W.-Y. Cheng, Opt. Lett. **36**, 76 (2011).
5. C.-Y. Cheng, C.-M. Wu, G.-B. Liao, and W.-Y. Cheng, Opt. Lett. **32**, 563 (2007).
6. M. Roberts, P. Taylor, S. V. Gateva-Kostova, R. B. M. Clarke, W. R. C. Rowley, and P. Gill, Phys. Rev. A **60**, 2867 (1999).
7. G. Hagel, C. Nesi, L. Jozefowski, C. Schwob, F. Nez, and F. Biraben, Opt. Commun. **160**, 1 (1999).
8. Those have been experimentally confirmed.
9. UTC, Coordinated Universal Time; TL, Telecommunication Laboratories of Taiwan.
10. F. Biraben, M. Bassini, and B. Cagnac, J. Phys. **40**, 445 (1979).
11. G. Grynberg, B. Cagnac, and F. Biraben, in *Coherent Nonlinear Optics*, M. S. Feld and V. S. Letokhov, eds. (Springer-Verlag, 1980), pp. 111–164.
12. B. Girard, G. O. Sitz, R. N. Zare, N. Billy, and J. Vigue, J. Chem. Phys. **97**, 26 (1992).
13. The authors of Ref. [1] used only one cell; S. Bergeson, Max-Planck-Institut für Quantenoptik, Hans-Kopfermann-Strasse 1, 85748 Garching, Germany (personal communication, 2013).